Fermi National Accelerator Laboratory

FERMILAB-Conf-87/137

Detector Dependent Contributions to Jet Resolution*

J. Freeman and C. Newman-Holmes
Fermi National Accelerator Laboratory
P.O. Box 500, Batavia, Illinois 60510

September 1987

*Presented at the Workshop on Experiments, Detectors, and Experimental Areas for the Supercollider, Lawrence Berkeley Laboratory, Berkeley, California, July 7-17, 1987.

Operated by Universities Research Association Inc. under contract with the United States Department of Energy

DETECTOR DEPENDENT CONTRIBUTIONS TO JET RESOLUTION

J. Freeman and C. Newman-Holmes

Fermi National Accelerator Laboratory[1], Batavia, IL

Abstract

We present results of calculations undertaken to study detector dependent effects that contribute to the energy resolution of jets. To accomplish this study, we have developed a fast, easily varied simulation of a generic 4π calorimeter. Physics processes used for benchmarks of performance were the transverse energy resolution of 1 TeV jets and the mass resolution of $W \rightarrow 2$ jets, for W's with 500 GeV transverse momentum.

1 Introduction

It is generally agreed that good measurement of jet energies is an important capability for any SSC detector. A variety of detector dependent effects contribute to jet energy resolution. These include calorimeter thickness, segmentation, energy resolution, electron/hadron response ratio and cracks or dead areas. The problems of energy carried off by neutrinos, overlapping events and limitations of jet reconstruction by clustering also affect jet energy measurements. Attempts to study a collection of effects such as these can easily become aimless rambles through a multi-dimensioned parameter space. Instead we approach the problem with a belief that many of the general features of these diverse effects can be studied with a relatively simple Monte Carlo program. We have written such a program incorporating parametrized showers and a very simple geometry. We describe the program below and present some results obtained with it.

2 Calorimetry Simulation

The calculations described herein were performed with a computer program interfaced to the widely used ISAJET event generation program [1]. A simple detector is simulated using several settable parameters. The detector consists of three regions: a spherical decay volume, an electromagnetic calorimeter and a hadronic calorimeter. Both calorimeters are spherical shells. The decay volume contains a cylindrical region where a solenoidal magnet field is present. The radius of the spherical decay volume is chosen to just enclose the cylinder, with the cylinder's size specified by the user. The radiation length, absorption length and thickness of each calorimeter are also settable.

The program goes through a list of particles made by ISAJET. For each particle, a distance to decay point, distance to electromagnetic conversion and distance to hadronic interaction are calculated using probablity distributions appropriate for the particle type. Particles are then tracked through the detector one by one. In the decay volume, a particle

[1]Operated by Universities Research Association under Contract with the U.S. Department of Energy

will decay if the distance to its decay point is less than the distance it travels through this volume. If a nonzero magnetic field has been specified, the particle's trajectory is appropriately changed.

When a particle reaches its predetermined shower or conversion point, parameters for its shower are generated. The shower parametrization has been described elsewhere [2]; longitudinal and transverse shower profiles as well as fluctuations are modelled. This parametrized shower is then integrated over the distance between the shower point and the calorimeter edge. If a shower starts in the electromagnetic calorimeter, the same shower is continued into the hadronic calorimeter. The electromagnetic/hadronic energy response is settable for each calorimeter. Note that in this model, a particle may not decay once its shower has begun. The total (electromagnetic + hadronic) energy deposited in the calorimeters is available for each particle both before and after smearing with a resolution function. The resolution is assumed to be of the form $\sigma_E/E = const/\sqrt{E} + 1\%$ where the constant is supplied by the user for each calorimeter (electromagnetic and hadronic) and the additional 1% is a systematic error associated with calibration. In addition, the energy is deposited in an η - ϕ array with specifiable segmentation. Energy is shared between the central tower (i.e., the one to which the particle track pointed) and its four nearest neighbors in η - ϕ space. The fraction of energy deposited in the central tower depends on the ratio of the shower size to tower size. The remaining energy is shared equally among the four nearest neighbor towers. Electromagnetic and hadronic calorimeter energies are saved separately in the η - ϕ array; only their sum is saved in the particle-oriented arrays. A simple clustering algorithm is used to find energy clusters in the η - ϕ array.

At a luminosity of 10^{33} cm^{-2}/sec, one expects an average of about 10 interactions in a 100 ns integration time. Our simulation includes an option to overlap minimum bias events with the generated events of interest. The average number of events to overlap may be varied. Then the actual number of overlapped interactions is determined for each event by sampling from a Poisson distribution with the specified mean.

3 Analysis

In this paper, we consider two benchmark measurements: The E_t distribution for 1 TeV jets, and the invariant mass distribution for 500 GeV P_t W's decaying into quarks which then hadronize into jets. The events were produced with version 5.2 of ISAJET. The jets were from TWOJET events with P_t constrained to be within the range 1000 - 1010 GeV, and θ 80° to 90°. The W's were produced by the WPAIR option, with θ between 80° and 90°, and the P_t range 450 - 550 GeV. After the events were created, the previously described simulation was used to generate calorimetry energy depositions. Clusters were then found in the calorimetry using a standard algorithm from CDF:

1. The set of towers with $E_t > 5.0$ Gev was determined. These were the seed towers for potential clusters.

2. For each seed tower not in a cluster, all nearest neighbor towers were searched, and any tower with $E_t > 1.0$ GeV was added to the cluster.

3. Neighbor towers of all towers in the cluster were searched, and any towers not in the cluster with $E_t > 1.0$ GeV were added. This step was repeated until no new tower was added to the cluster.

4. All clusters with centroids within $R < 0.7$ in η-ϕ space were merged into one large cluster, and the new cluster centroid was found. R is defined as:

$$R = \sqrt{((\phi_i - \phi_j)^2 + (\eta_i - \eta_j)^2)}$$

where i and j are cluster indices. For the jet E_t calculation, all energy within $R < 0.7$ of the cluster direction was summed.

The momenta of all final state partons (hadronizing) that fell within the 0.7 R cone were summed and the resultant E_t was calculated. This quantity was used as a normalization on an event-by-event basis. We felt that this choice of normalization separated the effects of gluon bremsstrahlung, and other "physics" processes from the effects of the actual detector performance.

It is interesting to see the difference between clustering, and summing all energy within the cone in η-ϕ space. Figure 1 shows the error in E_t measurement divided by the E_t of the hadronizing partons in the cone for two-jet events. Three curves are shown. The curve labelled "perfect" is obtained if one sums the energies deposited in the calorimeter for all daughter particles of the parton. This is clearly better than one can do in the real world where one doesn't know from which parton an observed particle is descended. The curve labelled "cluster" is obtained if one simply assumes the energies of the two highest P_t clusters are the parton energies. The curve labelled "cone" is obtained if one uses a reconstructed cluster to define a direction but then sums all energy within some distance in η - ϕ space to approximate the parton energy. The fact that "cone" is better than "cluster" indicates that there is energy from the parton which will not be included by a naive clustering algorithm.

To reconstruct the W invariant mass each tower within $R < 0.7$ was treated as a massless particle with all energy assumed to be deposited in the tower center, and the resultant invariant mass of this set of "particles" was calculated. We note that these calculations are very insensitive to the clustering algorithm used, since only the cluster direction is required. For the W analysis some additional cuts were applied to suppress problems in pattern recognition. The jets produced by the decay of 500 Gev W's are coalesced in our choice of calorimeter geometry. To ease pattern recognition, we chose events where no more than 25 GeV E_t of cluster energy was outside of the 2 leading clusters, and where the ratio of E_t's of the leading to the next to leading cluster was less than 1.25 . These cuts were typically 40 % efficient. The remaining events can in principle be used, but the pattern recognition is more difficult.

The curves shown below are from a sample of approximately 175 W's per case for the W analysis and 350 jets for the jet analysis.

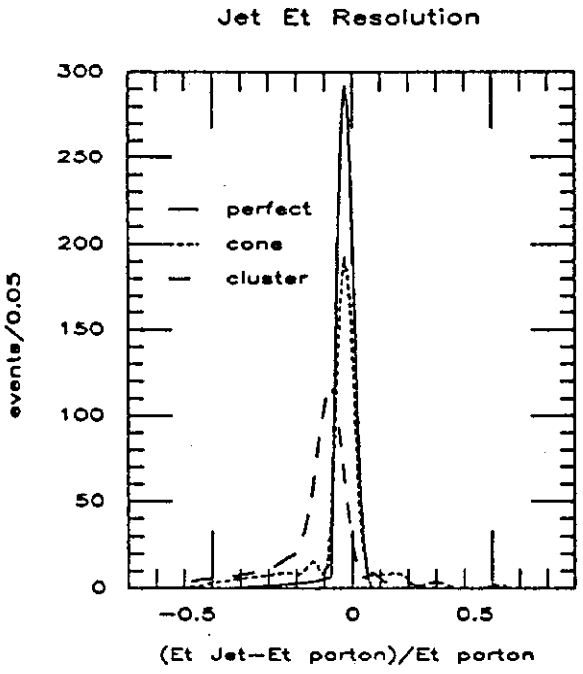

Fig. 1. Fractional Jet E_t resolution for various choices of pattern recognition.

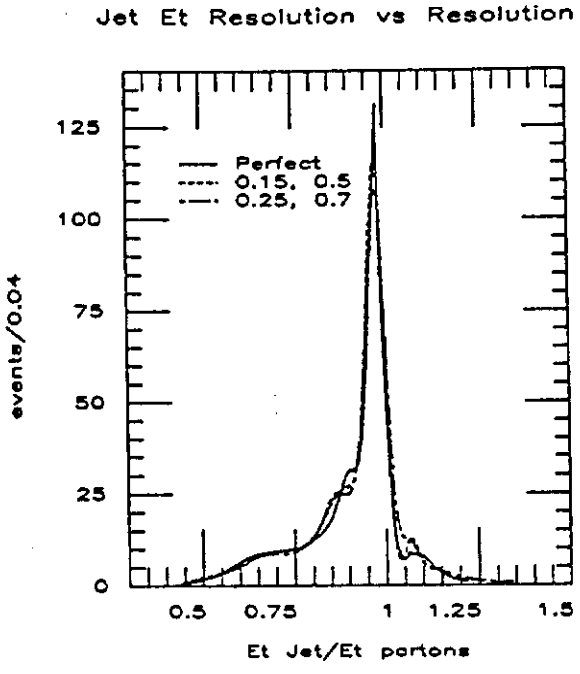

Fig. 2. Jet E_t resolution vs. calorimeter energy resolution.

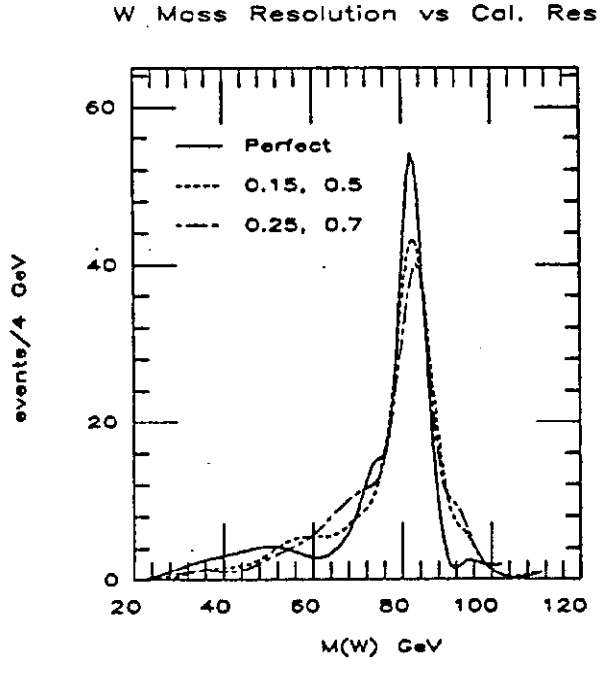

Fig. 3. W Invariant Mass resolution vs. calorimeter energy resolution.

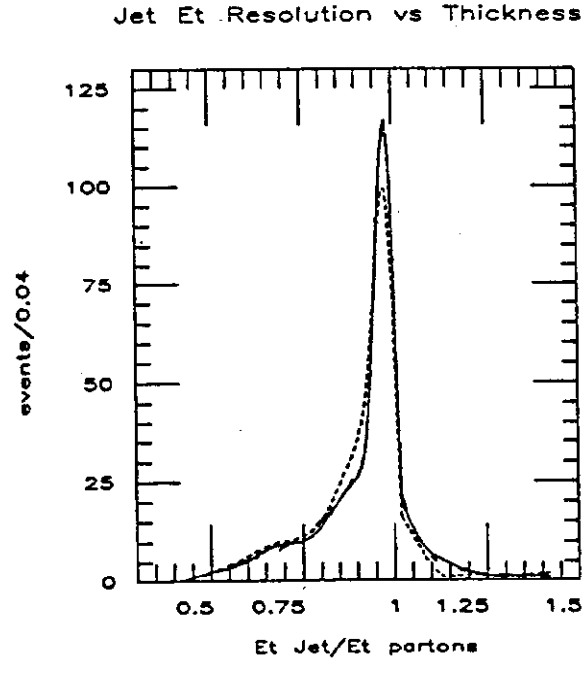

Fig. 4. Jet E_t resolution as a function of hadron calorimeter thickness in interaction lengths.

3.1 Dependence on Calorimetry energy resolution

Figure 2 shows jet E_t distributions for three choices of electromagnetic/hadronic calorimetry energy resolution. Numbers in the figure are to be divided by the $\sqrt{E}$ to determine the σ of the gaussian resolution for different energy depositions. There is no striking difference between the three cases, because the E_t resolution of a jet is determined by the E_t resolution of the leading particles, which, due to their high energy, are always well measured. The low energy tails of the distributions are due primarily to particles from the jet falling outside of the 0.7 R cone. The events in the tail may have a high energy parton lying close to the edge of the cone of $R < 0.7$. Particles from the hadronization of this parton often land outside of the cone. In a sense, this tail is an artifact of the jet definition.

Figure 3 shows W mass resolution for the three cases. Here we see that calorimeter resolution is more important than in the jet case. Low energy particles in the lab frame can make large contributions to the invariant mass calculation. It is important to measure these particles accurately.

3.2 Dependence on Hadron calorimeter thickness

Figure 4 shows the E_t distribution for 1 TeV jets as a function of the thickness in interaction lengths of the hadron calorimetry. In all cases the electromagnetic calorimeter in front of the hadron calorimeter is assumed to be 17 radiation lengths, and 0.8 interaction lengths thick. The curves for 10 and 15 interaction lengths are indistinguishable. The distribution for five interaction length thick hadron calorimetry shows a slightly worse resolution, and a slight low energy tail from leakage. The effect of calorimetry thickness would be more pronounced in the forward/backward regions, where the particle energies (for a fixed E_t) are larger. Figure 5 shows the results for the mass distribution of W's. In this case there is no difference between any of the three cases. This is partially caused by the cuts that define the event sample. The requirement of cluster E_t balance suppresses events where there is substantial leakage or punchthrough. In addition, the jets from the W decay are softer, again reducing the effect of leakage.

3.3 Dependence on Intrinsic E/H Response ratio

Hadronic shower energy deposition has two components. A fraction of the energy goes into π_0s and is deposited like electromagnetic showers. The remaining energy is deposited by ionizing hadrons. The ratio of calorimetry response per GeV of shower energy for these two types of energy deposition is called the intrinsic E/H ratio. It is in general not equal to 1.0 [3].

Figure 6 shows the jet E_t distributions for three values of the intrinsic E/H ratio. We note that there is a broadening of the distribution as the ratio varies away from 1.0 The curves for 0.8 and 1.2 are not very different. In general, E/H not equal to 1.0 causes a nonlinearity of response for different energy jets. Figure 7 shows the observed E_t fraction versus jet E_t for 2 choices of E/H, normalized to E/H = 1. Coincidentally, the curves intersect at about 1 TeV, explaining the lack of shift of the peaks of the distributions

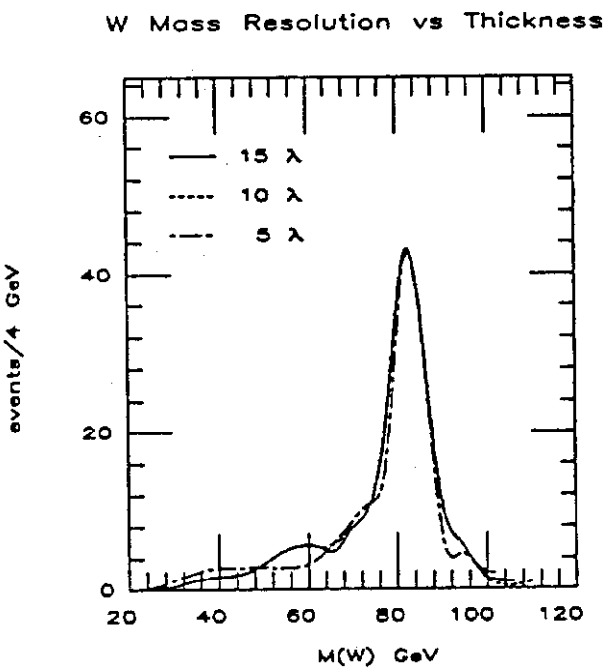

Fig. 5. W mass resolution as a function of hadron calorimeter thickness.

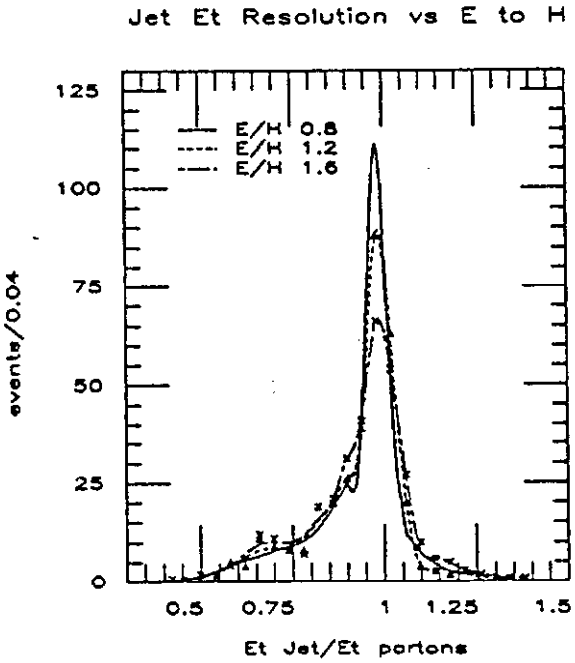

Fig. 6. Jet E_t resolution vs. intrinsic E/H ratio.

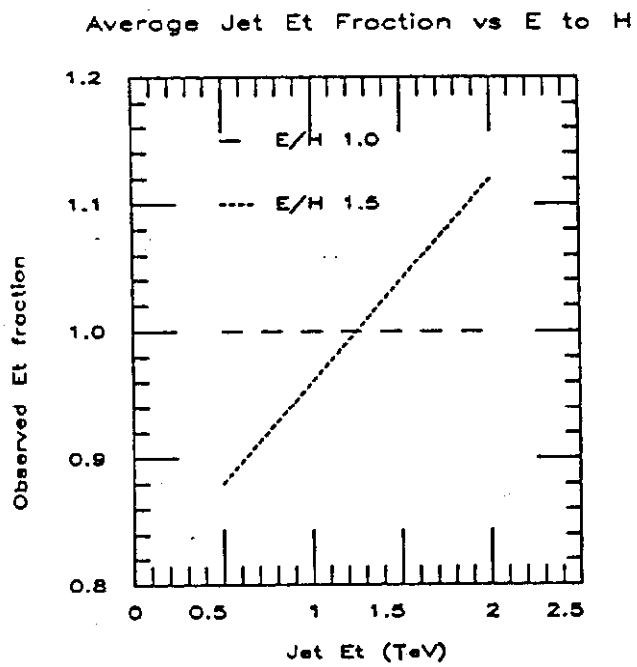

Fig. 7. Average jet E_t fraction as a function of jet E_t for different values of E/H.

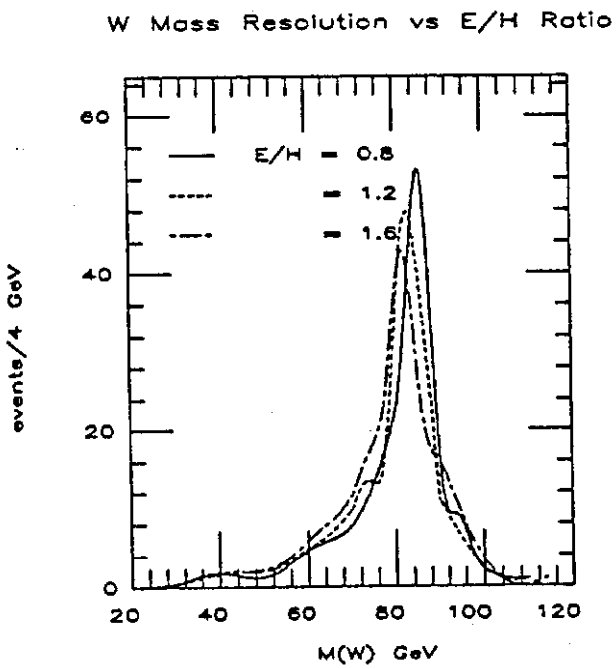

Fig. 8. W mass resolution vs. calorimetry E/H.

in Figure 6. This nonlinearity can be a serious problem for measurements of energy distributions. Figure 8 shows the effect of varying E/H on the W mass distribution. We see an increase of the width and a systematic shift of the peak energy.

3.4 Dependence on Calorimeter Tower Size

Here we consider the effect of different tower sizes. The towers are rectangular cells in η-ϕ space. The only effect tower size can have on jet E_t resolution is from mismeasure of the θ direction of energy flow, causing an error in the $\sin(\theta)$ weighting for the E_t calculation. At θ approximately 90°, this is a very small effect for any reasonable tower size. In our invariant mass algorithm, the tower size is very important. All energy deposited in a tower is assumed to come from the tower center, so the larger the tower, the larger the possible error in direction determination of the energy flow into the tower. Figure 9 shows W invariant mass distributions for three cases of tower size: $\delta R = 0.01$, 0.03, and 0.1 . The mass resolution is significantly worse with the largest tower size.

3.5 Dependence on Solenoidal Magnetic Field

Since jet E_t resolution is determined primarily by the stiff leading particles, magnetic field in the central tracking volume has very little effect. The W invariant mass distribution is somewhat affected by the applied magnetic field, with a broadening at larger fields. The central tracking volume was 1.4 meters in radius for these studies. Figure 10 shows the change in the shape of the W invariant mass distribution for 3 choices of magnetic field.

We note that many of the SSC detector designs under consideration have at least some of the calorimetry inside the magnetic field. Problems this may cause are not addressed by our simulation.

3.6 Dependence on Additional Events in the Detector Resolving Time

In this study, we consider the effect of additional background events which fall within the detector resolving time of the signal events. For the background events, we used ISAJET TWOJET events with jet P_t's between 3 and 15 GeV. This corresponds to about 150 millibarns of cross section at 40 TeV, so it should be a reasonable model for the background. The jet E_t resolution is unaffected by these soft events. The W mass resolution has a very striking sensitivity to the number of superimposed background events as shown in Figure 11. The curves correspond to the distribution for the signal events, and for the signal events with a number of superimposed background events. The number of background events is extracted on an event-by-event basis from a Poisson distribution with a mean of either three or 10 events.

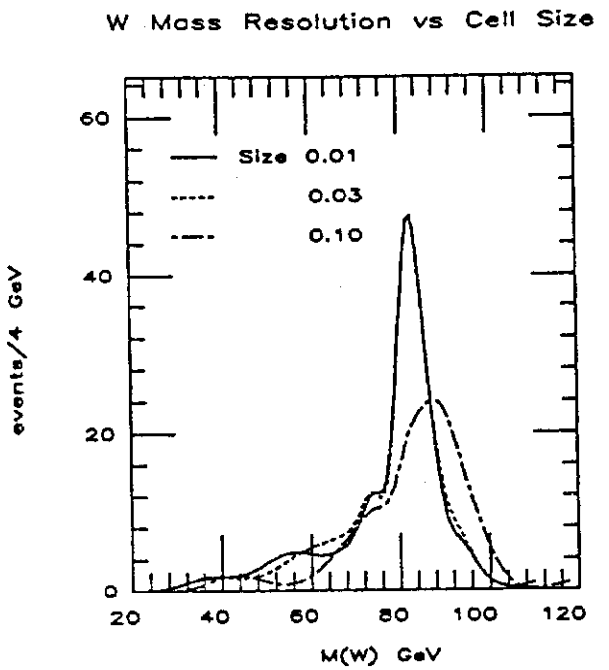

Fig. 9. W mass resolution vs. calorimeter tower size in $\eta - \phi$.

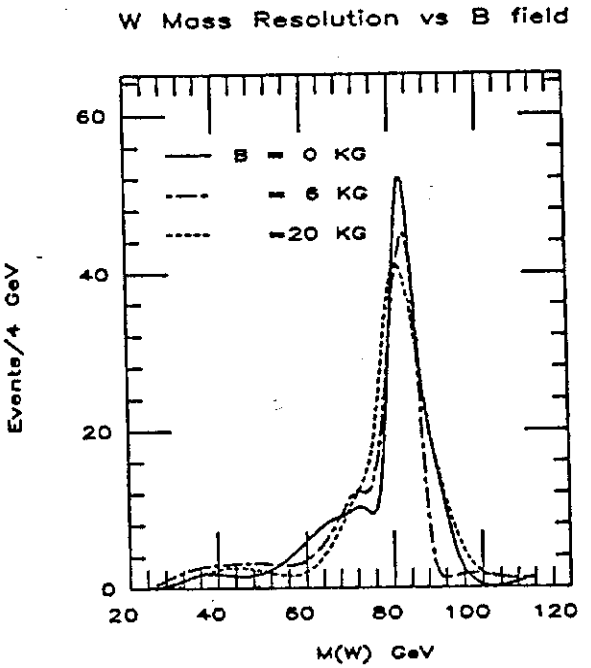

Fig. 10. W mass resolution as a function of magnetic field.

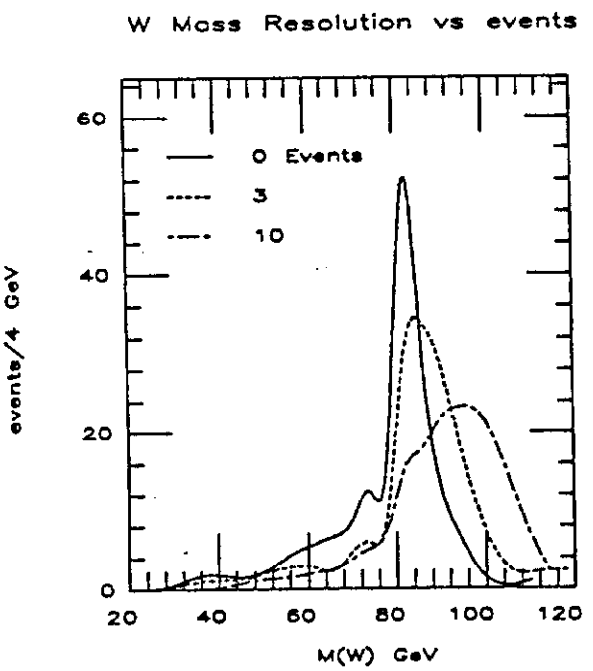

Fig. 11. W mass resolution vs number of superimposed background events.

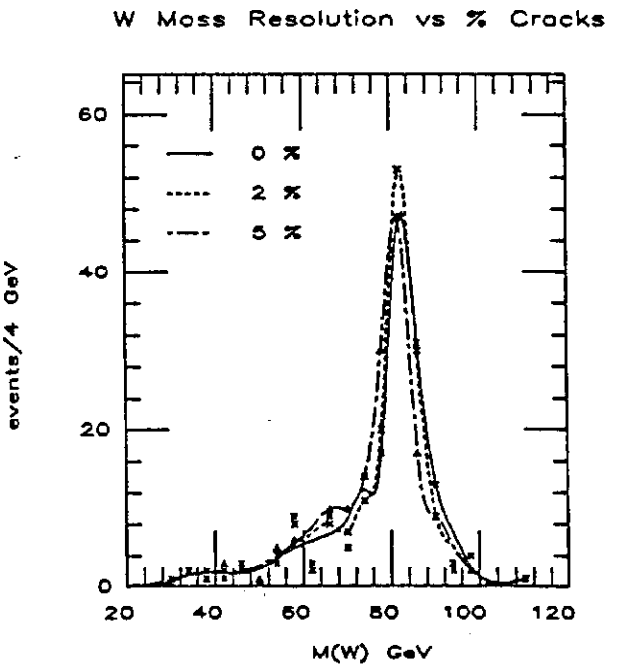

Fig. 12. W mass resolution for different percentages of cracks.

3.7 Dependence on Dead/Crack Regions

We adopted an ad hoc procedure to investigate the effect of dead material and cracks. Each tower was given a fixed percentage of dead area. Particles landing in the dead portion of the tower had the energy that they were to deposit into the calorimetry reduced by a factor of 2. Figure 12 shows W mass distributions for 0%, 2%, and 5% dead areas. There is surprisingly little effect.

4 Conclusions

We have used a simple Monte Carlo program to investigate several contributions to jet energy resolution. We summarize our conclusions about each of the effects considered:

1. Calorimetry Resolution: The jet E_t signal is independent of the calorimetry energy resolution. The W invariant mass signal however does have some dependence. Accurate measurement of low energy particles is important.

2. Calorimetry Thickness: Neither signal is particularly sensitive to the thickness of the hadron calorimeter in interaction lengths. Higher energy jets would have more degradation due to leakage. Missing E_t signatures are the most sensitive benchmark to determining the desired thickness.

3. Both signals are sensitive to the E/H ratio. Since there is an understanding of this ratio, and the ability to tune it, there is no reason to build calorimetry with E/H far from 1.0 . The range 1.1 to 0.9 is acceptable.

4. Tower Size in η-ϕ: The jet signal is almost totally insensitive to tower size, an expected result. The W invariant mass is very sensitive to the choice. A tower size of 0.03η x 0.03ϕ is acceptable. Increasing the size to 0.1 x 0.1 seriously degrades the W mass resolution.

5. B field: The jet E_t distribution is insensitive to the field. The W mass resolution is affected somewhat. 30 kG-m of field causes about a factor of 1.5 broadening of the peak of the mass distribution.

6. Number of Background Events in the Detector Resolving Time: The W mass distribution is very sensitive to the presence of additional background events. The presence of even three additional events causes a serious worsening of mass resolution.

7. Dead Areas. Dead areas at the level of a few percent have little effect on either distribution. It is very difficult to generalize about cracks, since the exact details of their properties must be known to determine their effect. Missing E_t measurements are probably most sensitive to the effects of cracks.

References

1. F.E. Paige and S.D. Protopopescu, 1982 DPF Summer Study, Snowmass, CO, June 1982, p. 471.

2. J. Freeman and A. Beretvas, 1986 DPF Summer Study, Snowmass, CO, June 1984, p. 482

3. R. Wigmans, CERN/EF 86-18, Sept.,1986